

# Report on preliminary calibration of outputs released by the MT

Sub-action B2.1

31.03.2022



## Content

<b>Introduction .....</b>	<b>2</b>
<b>The app PocketDRIVE.....</b>	<b>2</b>
<b>Tool development and functionalities.....</b>	<b>2</b>
<b>Preliminary calibration of thresholds of early water stress .....</b>	<b>6</b>
<b>STARWARS application for the 6 Demo Farms: specific modelling solution (UNIPV) .....</b>	<b>10</b>
<b>Model description.....</b>	<b>10</b>
<b>Input data preparation.....</b>	<b>12</b>
<b>Model calibration.....</b>	<b>15</b>
<b>Model results .....</b>	<b>15</b>
<b>References .....</b>	<b>19</b>
<b>STARWARS Model Application referreces .....</b>	<b>19</b>

## Introduction

The objective of Task B2.1 was to provide a preliminary calibration of the monitoring tool (MT) that is being developed to support farmers in:

- quantitatively evaluating the soil water storage at the beginning of the season;
- following and tracking the seasonal soil water depletion;
- detecting and validating early thresholds of significant water stress.

To reach these aims, the MT includes three components (Fig. 1):

1. a geo-referenced database with soil and weather data;
2. a modelling solution for estimating the soil water content at the beginning of the season and for daily calculation of water balance;
3. a dedicated smart-app (PocketDRIVE), to allow the user easily interacting with the MT.

This deliverable is focused on describing and reporting the results of the first year calibration of (i) the app PocketDRIVE and (ii) the modelling solution based on the model STARWARS and the geo-referenced database of soil and weather data.

## The app PocketDRIVE

### Tool development and functionalities

The smartphone app PocketDRIVE has been developed to provide a clear and user-friendly interface while enabling a close interaction between the user and the MT (**Fig. 1**). By using PocketDRIVE indeed, it is possible to receive information on early warnings of water stress in specific vineyards and suggestions to manage water scarcity conditions, but also to actively supply information to the MT by:

1. creating a registry of the farm's vineyards, by providing their GPS position as well as information on the cultivar, training system, etc.;
2. providing key data for refining the calculation of the daily water balance (i.e., leaf area index of the vineyard and of the inter-row grasses, as well as management events affecting the amount of vegetation like, e.g., green pruning);
3. verifying early warnings of water stress by analysing canopy architecture.

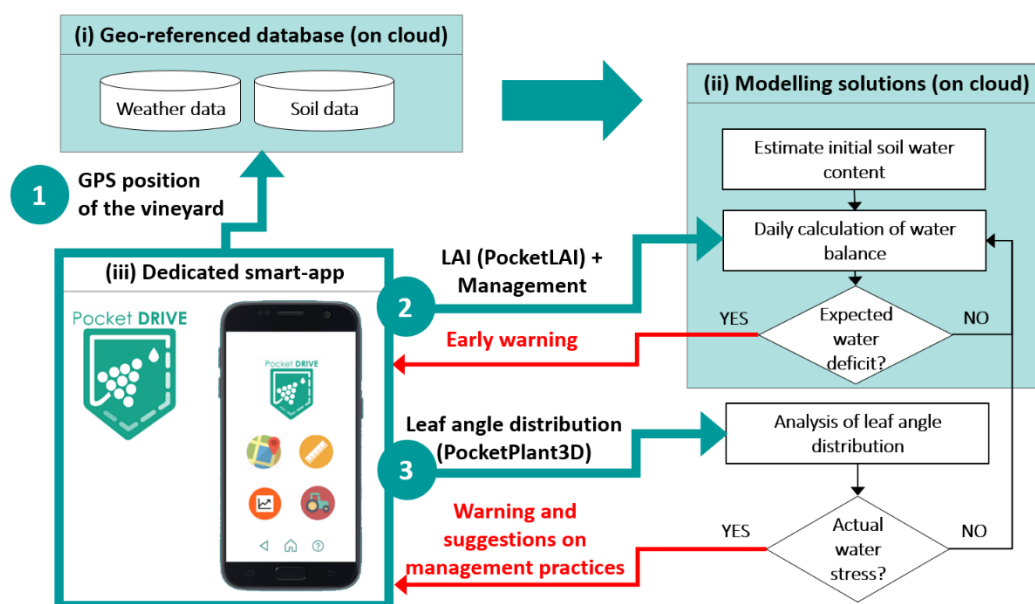


*Figure 1.* Description of the monitoring Tool (MT), with indications about the three main functionalities provided by the app PocketDRIVE. This app has been specifically developed to allow the user interacting with the MT by both providing (green arrows) and receiving (red arrows) information.

Given the key role of the tool usability, a mockup of the app was presented and discussed with the farmers and other project partners during dedicated events of co-development (Action B3; meeting held on November 25<sup>th</sup>, 2021) and project meeting (December, 2<sup>nd</sup>, 2021). The mockup of the app was made available online (<https://framer.com/share/PocketDRIVE--dJ1101MyYANvI9xsgFsB/al5D4uxyy>), to enable farmers and project partners to access it at any time and directly from their own smartphone, to allow a better simulation of the user experience and the provision of effective feedbacks.

The app was refined according to the feedbacks received, and it is now available to project partners for use during the season 2022. Here below a description of the app main functions.

By clicking on the top-left icon of the main screen of PocketDRIVE (Fig. 2a), it is possible to access its first main functionality (creating the registry of vineyards, Fig. 2b). From here, the user can enter the name to be used within the MT to identify the vineyard, the cultivar, the training system, the inter-row space, how the inter-row is managed (e.g., bare soil, cover crops, etc.), and the vineyard's GPS coordinates (by drawing its area through a dedicated touch-screen function; Fig. 2c). Such information needs to be entered just once during the app configuration. Nevertheless, it is always possible to delete a vineyard from the registry or modify the information associated to it (e.g., change the inter-row management system, Fig. 2b). Once the vineyard is registered, a text file (.csv) with all the information is automatically created and sent to the MT on cloud. All these data are indeed needed to retrieve geo-referenced soil and weather data and estimate the vineyard's water balance.

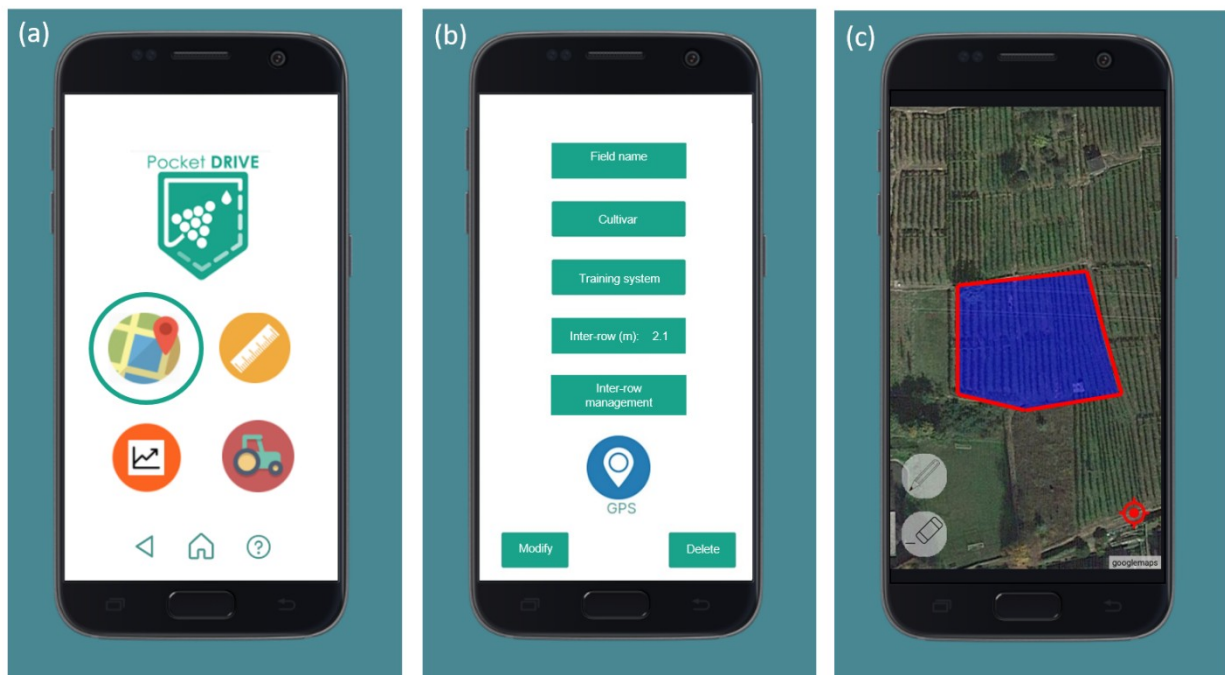


Figure 2. Screenshots showing how to create a vineyard in the app. Icon to access this functionality (a); information that needs to be specified (b); definition of the vineyard GPS position by simply drawing its borders on the map (c).

Concerning the second functionality (providing data for refining the calculation of the daily water balance, Fig. 1), from the top-right icon (Fig. 3a) the user can provide the MT with estimates of the leaf area index (LAI) of both the vineyard and the inter-row grasses (Fig 3b). PocketDRIVE implements the approach developed by Confalonieri et al. (2013) to estimate leaf area index by using the camera and accelerometer of common smartphones. This approach has been widely tested on different crops (Campos-Taberner et al., 2016, Francone et al., 2014) including adaptation to vineyards (Orlando et al., 2016). After acquisition (when the user clicks on the button "Update measurements"; Fig. 3b), LAI data are automatically sent to the MT on cloud, where they are used to refine the water balance estimate.

More in detail, the water balance automatically simulates the phenological development of grapevine (Mariani et al., 2012, Cola et al., 2014, Cola et al., 2017), distinguishing among five different ripening classes of cultivars (early, early-mid, mid, mid-late, late) (Calò et al., 2017). The daily maximum evapotranspiration of grapevine is obtained by applying the multiplicative factor  $k_c$  to the reference crop evapotranspiration  $ET_0$  (Allen et al., 1998), being  $k_c$  a function of the

phenological stage and the consequent development of grape canopy (Cola et al. 2014), determining the fraction of intercepted incoming global solar radiation (Riou et al., 1989).

Inter-row cover is also considered in order to define the inter-row evapotranspiration.

LAI direct measurements are used to:

- correct the simulated value of the fraction of intercepted incoming solar radiation
- correct the phenological stage of grapevine

As described in detail in Confalonieri et al. (2013) and Orlando et al. (2016) the acquisition of the LAI measurements is quick and suitable for operational contexts. Basically, the user has to click at the center of the screen to activate the measuring mode (Fig.3c). PocketLAI automatically takes images of the canopy at a view angle of 57.5° while the user is rotating the device along its main axis. The gap fraction is derived using a fully automatic segmentation algorithm specifically developed to detect the sky pixels according to their chromatic values in a Hue- Saturation-Brightness (HSB) color space. The LAI value is then retrieved according to the light transmittance model described by Baret et al. (2010) and, in case of vertical canopies, by using also the inter-row distance (Orlando et al., 2016) that is provided by the user while registering the vineyard (Fig 2).

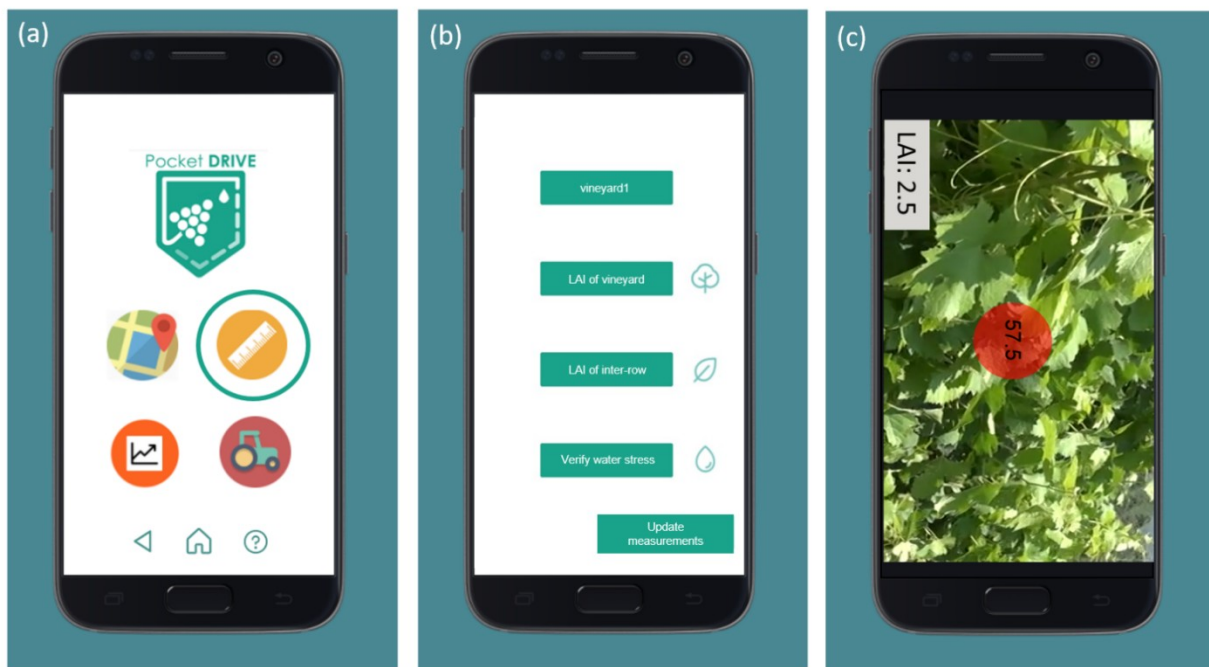


Figure 3. Screenshots of PocketDRIVE showing how to collect estimates of leaf area index (LAI) of the vineyard. Icon to access this function (a); screen where it is possible to specify the vineyard in which the measurement are being collected and the kind of measurement (i.e., LAI of the vineyard and/or LAI of the inter-row grasses) (b); measuring mode for LAI estimates (c). The inclination of the device is shown in the red circle in the middle, with the app automatically acquiring images at 57.5° whiel the device is rotated along its main axis.

The estimation of the daily water balance can be refined also by considering management events that affect the amount of vegetation in the vineyard. This includes green pruning of the grapevines, as well as management of the inter-row such as soil tillage, grass cutting, grass smashing, etc. Information about these management events ca be provided to the MT through the PocketDRIVE bottom-right icon (Fig. 4a) that opens a dedicated screen where the type of intervention and the date can be entered (Fig. 4b). A text file (.csv) with all the management information is automatically created and sent to the MT on cloud.

Given that the weather database includes forecasted data, the daily water balance is estimated also for the five days ahead in order to provide early warning of water stress. In case drought is expected, in this first version of the app an alert is sent to the user as a text message (SMS) and/or an email (according to the user's preferences). After the first season of tests (season 2022) the interaction with the demo farmers and the living labs will allow to identify the most suitable and effective way to provide users with water stress warnings, to be included in the final (release) version.

When the user receives an alert, the actual occurrence of water stress conditions can be verified with the app by measuring variations of canopy architecture that, in turn, are related with drought occurrence. PocketDRIVE implements the app PocketPlant3D (Confalonieri et al., 2017), which uses the device accelerometer and magnetometer to measure the angles of leaf surfaces with respect to the zenith while the device is moved along the leaf main axis. Leaf angles are then used to automatically estimate synthetic indices of canopy architecture like the X parameter of the Campbell' ellipsoidal distribution (Confalonieri et al., 2017). This index has proved to properly describe canopy architecture, with low values indicating erectophile canopies and high values corresponding to a planophile behaviour. By clicking on the icon for collecting measurements (Fig 3a) and on that for verifying water stress (Fig. 3b), the user can easily start collecting leaf angles while keeping the device parallel to the leaf main axis (Fig. 5a). To ensure high usability during leaf angles collection, the user can start and stop the recording by simply clicking at the center of the device' screen (Fig 5c). It is also possible to remove measurements in case of error. The app keeps the counts of the number of leaves measured (Fig 5d). Preliminary results of field tests conducted during 2021 suggested indeed that around ten leaves randomly selected in the middle part of the canopy (Fig. 5b) are enough to provide an accurate evaluation of canopy architecture. Therefore, if less than 10 leaves have been measured the app does not allow to verify water stress and shows instead a message suggesting to collect more data.

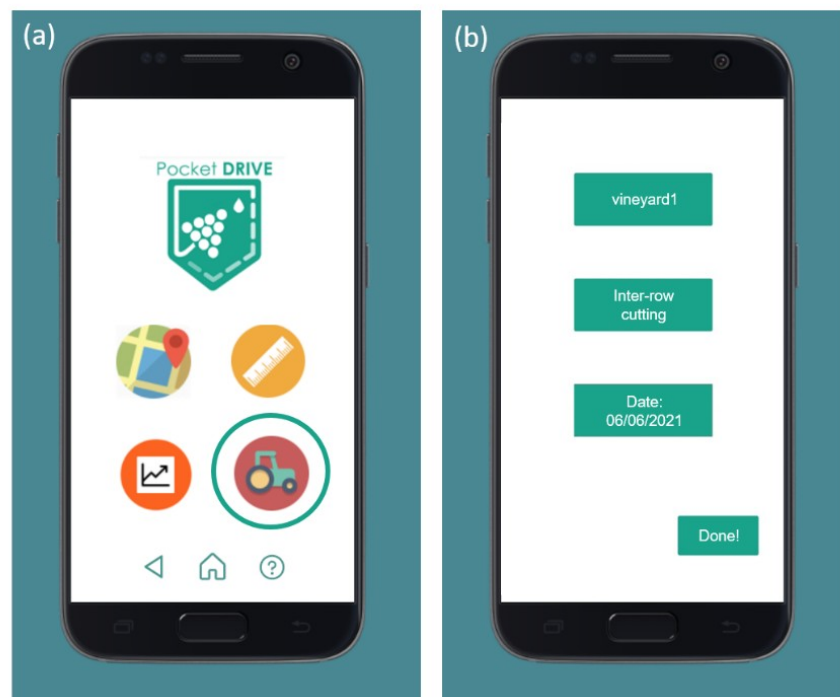


Figure 4. Icon (a) and main screen (b) to register management events.

Once the angle collection is complete, the user can verify the occurrence of water stress by clicking on the dedicated button ("Verify water stress", Fig. 5c). The app automatically estimates the values of X, makes the comparison with threshold values indicating the onset of water stress (details about thresholds calibration are provided in the next section of this document), and returns a quick response in terms of stress level (no/moderate/severe stress). In case stressful conditions are actually occurring, the app provides a warning together with bullet-point suggestions on management practices that can be undertaken to cope with drought (e.g., kaolin spraying). A detailed guide about management practices useful to mitigate the effects of water stress is instead provided together with the app documentation.

Lastly, all the information collected with the app (LAI and canopy architecture measurements, management events) can be accessed and verified by the user through the orange bottom-left icon (Fig. 4a).

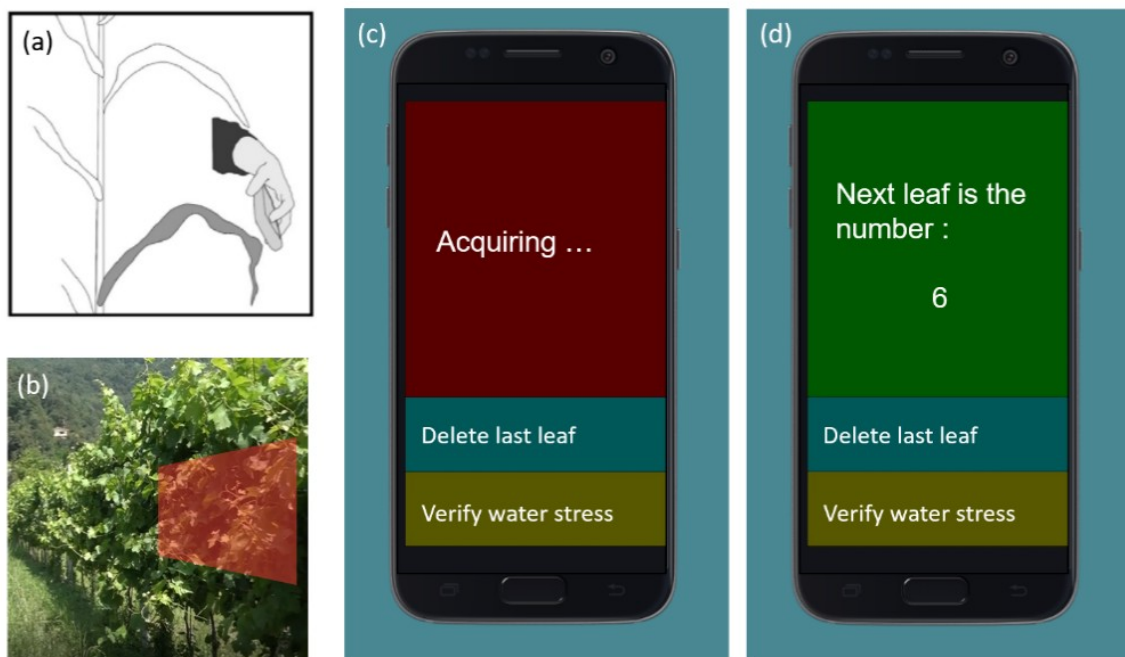


Figure 5. Collection of leaf angles to evaluate canopy architecture and verify water stress occurrence. The device should be kept parallel to the leaf main axis (a). The angle collection should involve leaves in the middle part of the canopy (b) and can be started by clicking on the red button (c). It is possible to delete measurements in case of errors. The app keeps count of the leaves measured (d) because at least 10 leaves are needed to derive reliable estimates of canopy architecture.

## Preliminary calibration of thresholds of early water stress

Dedicated field activities were conducted during 2021 to derive a first calibration of the relationships between canopy architecture and plant water status.

Three sampling events (June 21, July 30, and August 10) were carried out in one vineyard in Ziano Piacentino (PC) where the cultivar Croatina was grown, whereas two sampling events (June 21, and August 10) were conducted in one vineyard in Castel San Giovanni (PC) with the cultivar Malvasia. For the latter vineyard, field measurements on July 30 were not possible because of bad weather conditions.

Measurements of plant water status and canopy architecture were conducted at five points for each vineyard during the field visits with no water stress (i.e., June 21 and July 30), and at 9 points for each vineyard during the last sampling (August 10, marked water stress), to better capture the within-field variability in plant water status.

Physiological measurements of plant water status were conducted by using a portable gas exchange analyser (ADC Biosystems) – for evaluating stomatal conductance ( $g_s$ ,  $\text{mmol m}^{-2} \text{s}^{-1}$ ) and transpiration ( $E$ ,  $\text{mmol m}^{-2} \text{s}^{-1}$ ) – and a pressure chamber, to measure leaf water potential ( $\Psi_L$ , MPa). Canopy architecture was evaluated by using the app PocketPlant3D (as implemented in PocketDRIVE) to collect the angles (i) of the same leaves on which physiological measurements of water status were acquired and (ii) of additional leaves sampled in the same area (around 20 additional leaves, on average). These additional samplings were carried out to define a protocol of acquisition that provides the best compromise between a small number of leaves to be measured and a high accuracy of canopy architecture estimates. All measurements were conducted around midday. Overall, 124 leaves were sampled for physiological measurements, and more than 650 leaves for canopy architecture.

Leaf angles collected with PocketPlant3D ( $\theta_L$ ) were used to estimate two synthetic indices of canopy architecture: the parameter  $\chi$  (unitless) of the Campbell's ellipsoidal leaf angle distribution (Campbell, 1990; Eq. 1) and the light extinction coefficient of solar radiation ( $k$ ; Eq. 2) (Campbell, 1986).

The parameter  $\chi$  represents the ratio between the horizontal and the vertical semi-axis of an ellipsoid, thus providing a synthetic representation of the degree of erectness of the photosynthetic tissues (Campbell, 1986, 1990). The lower the value of  $\chi$ , the higher the tendency of the distribution to approximate a prolate spheroid (erectophile canopy).

The parameter  $\chi$  is estimated as follows:

$$\chi = -3 + \left(\frac{MTA}{9.65}\right)^{-0.6061} \quad (1)$$

Where MTA is the mean tilt angle (rad), estimated as the complementary of  $\theta_L$  because it represents the angle between the normal to the screen and the zenith (Campbell, 1990).

The extinction coefficient for solar radiation ( $k$ , unitless) was then estimated by using the parameter  $\chi$  according to Eq. 2 (Campbell, 1986):

$$k = \frac{\sqrt{\chi^2 + \tan^2 \theta_L}}{A} \quad (2)$$

Where  $A$  was calculated as proposed by (Campbell, 1990):

$$A \approx \chi + 1.774 (\chi + 1.182)^{-0.733} \quad (3)$$

Relationships between the values of  $\chi$  and  $k$  and physiological variables describing crop water status (stomatal conductance, transpiration, and leaf water potential) were evaluated through linear regression. These relationships were then used to derive the threshold values of  $\chi$  and  $k$  corresponding to a stomatal conductance of  $200 \text{ mmol m}^{-2} \text{ s}^{-1}$  (threshold for moderate stress) and  $100 \text{ mmol m}^{-2} \text{ s}^{-1}$  (threshold for severe stress).

There is general consensus in the literature that well-watered vines have midday  $\Psi_L$  values of about -7 bar and  $g_s$  values higher than  $300 \text{ mmol} \cdot \text{m}^{-2} \cdot \text{s}^{-1}$ , moderately stressed vines have midday  $\Psi_L$  values of about -10 bar and  $g_s$  values close to  $200 \text{ mmol} \cdot \text{m}^{-2} \cdot \text{s}^{-1}$ , and severely-stressed vines have  $\Psi_L$  lower than -12 bar and  $g_s$  lower than  $100 \text{ mmol} \cdot \text{m}^{-2} \cdot \text{s}^{-1}$  (e.g., Williams and Araujo 2002; Bellvert et al., 2014).

Results showed that the three sampling events allowed to cover a wide range of crop water status, with conditions close to optimum during the first field visit, and water stress increasingly higher while moving through the summer. Observed stomatal conductance values ranged between  $43 \text{ mmol} \cdot \text{m}^{-2} \text{ s}^{-1}$  and  $330 \text{ mmol} \cdot \text{m}^{-2} \text{ s}^{-1}$ , whereas  $\Psi_L$  varied from -13.5 bar to -9 bar.

In general, a good agreement was found between plant water status and canopy architecture, without clear differences due to the index of canopy architecture used (parameter  $\chi$  or light extinction coefficient). For this reason, results are hereafter discussed only for the first index ( $X$ ), being the light extinction coefficient derived from it (Eq. 2).

Figure 6 shows the relationships found between canopy architecture and variables describing plant water status by considering measurements from single plants of Croatina and Malvasia. Figure 7 shows instead the same relationships but (i) with values averaged for each combination sampling date  $\times$  inter-row treatment and (ii) with parameter  $\chi$  derived by including additional random leaves to those used for physiological measurements, because these are the final relationships used to define the thresholds of  $X$  (Table 1).

Figure 7 shows how for cultivar Croatina there are 3 points (corresponding to the three field visits), because the entire vineyard has the inter-row space managed with spontaneous grass kept slashed throughout the season. In the vineyard with Malvasia, instead, alternative management practices of the inter-row were under evaluation (i.e., bare soil, temporary cover crop smashed and piled up on the row, mulching of the mid-row by rolling the temporary cover crop). Therefore, in this case there are 4 points because the values from the first sampling were averaged together (the entire vineyard was under optimal water conditions), whereas in the second sampling event (August 10, marked water stress) plant water status and canopy architecture were evaluated separately for each of the three treatment.

Results highlighted a better agreement for Malvasia as compared to Croatina (Fig. 6) for both stomatal conductance and transpiration, although the relationships were always highly significant ( $p$ -value  $< 0.001$ ). Similar results were found for leaf water potential (Fig. 6e-f) but with low values of  $R^2$  in this case.



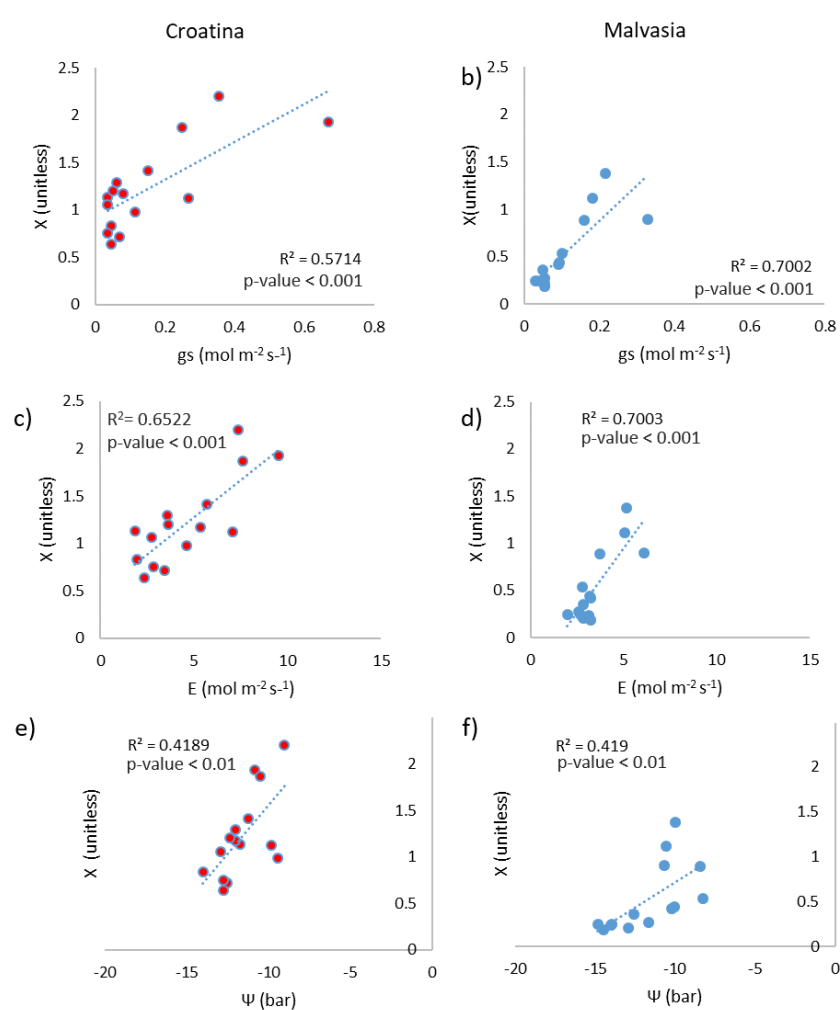


Figure 6. Relationships between the X parameter of the Campbell's elipsoidal distribution (a synthetic index of canopy architecture) and physiological variables of plant water status: stomatal conductance (a, b); transpiration (c, d) and leaf water potential (e, f). All the measurements were collected at midday. Cultivars: Croatina (red dots, left panels) and Malvasia (blue dots, right panels). Each dot represents the average of the measurements taken on the same plant, with measurements of canopy architecture and of plant water status conducted on the same leaves.

Considering relationships based on average values for each combination sampling date × inter-row treatment (Fig. 7), the best results were achieved for both stomatal conductance and transpiration, whereas leaf water potential shows lower  $R^2$  values, especially for Croatina.

This led to use the relationships between X and stomatal conductance to derive the thresholds values of X corresponding to the onset of water stress. The calibration curves obtained are reported in Table 1, together with the X values representing thresholds for moderate and severe water stress. These thresholds are those currently implemented in the first version of PocketDRIVE.

The variability observed between the calibration curves obtained for Croatina and Malvasia led to retain cultivar-specific calibration curves at this stage. Merging the data of the two cultivars led indeed to a marked reduction of  $R^2$ .

Nevertheless, data from the 2022 season will allow to derive more robust relationships and evaluate the actual need of cultivar-specific calibration curves.

The activities conducted for this preliminary calibration also allowed to define a protocol for canopy architecture measurements. The analysis of of the data collected with the app showed indeed how the angles of around ten leaves are enough to derive reliable estimates of canopy architecture, thus confirming the suitability of this approach for water stress evaluation for operational contexts (only few minutes are needed for conducting these measurements, few seconds per leaf).

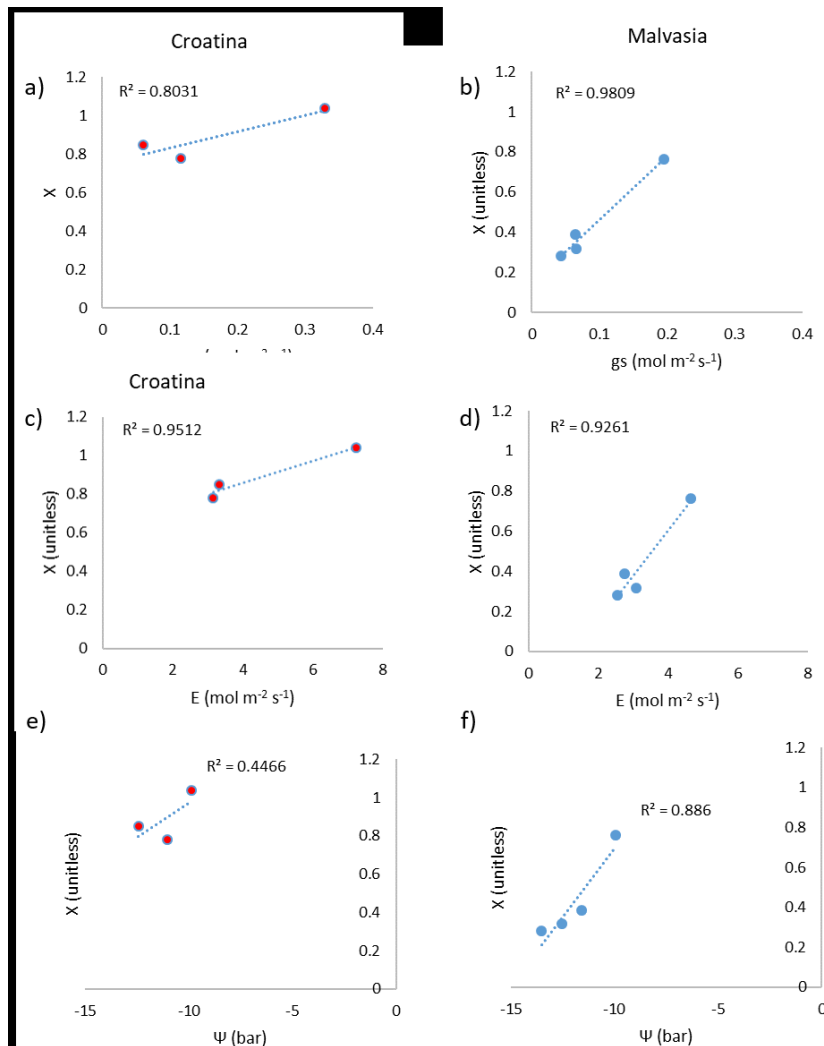


Figure 7. Relationships between the X parameter of the Campbell's ellipsoidal distribution (a synthetic index of canopy architecture) and physiological variables of plant water status: stomatal conductance (a, b); transpiration (c, d) and leaf water potential (e, f). All the measurements were collected at midday. Cultivars: Croatina (red dots, left panels) and Malvasia (blue dots, right panels). Each dot represents the average of each combination sampling date × inter-row treatment.

Table 1. Calibration curves derived from field data collected in 2021 to identify the threshold values of X corresponding to a stomatal conductance of  $0.2 \text{ mol m}^{-2} \text{ s}^{-1}$  (onset of moderate water stress) and of  $0.1 \text{ mol m}^{-2} \text{ s}^{-1}$  (onset of severe water stress). These relationships are also shown in Fig.7 a and 7b.

Cultivar	Calibration curve	Threshold value of X	
		Moderate stress	Severe stress
Croatina	$X = 0.8452 \cdot gs + 0.7478$ ; $R^2 = 0.80$	0.92	0.83
Malvasia	$X = 3.1578 \cdot gs + 0.1459$ ; $R^2 = 0.98$	0.78	0.46

# STARWARS application for the 6 Demo Farms: specific modelling solution (UNIPV)

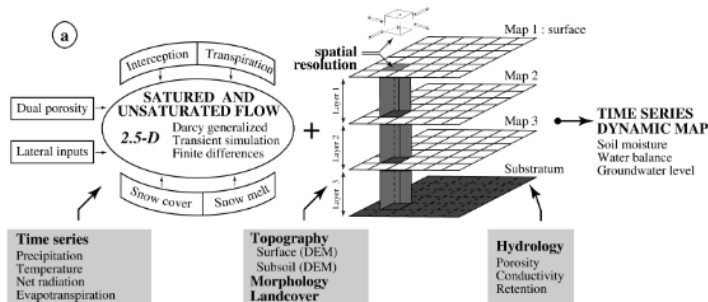
## Model description

For the site-specific modelling of the hydrological dynamics of the 6 test sites we applied the the STARWARS (Storage and Redistribution of Water on Agricultural and Revegetated Slopes) model (Van Beek, 2002). In 1999, Van Beek and Van Asch proposed a spatially distributed physically based model coupling hydrological and stability dynamics. The model consists of a core model describing the dynamics of saturated and unsaturated flow in the soil and of sub-models that describe related hydrological processes such as interception, transpiration, and snow accumulation and snow melt. The core model represents the soil column, typically consisting of three layers, overlying semi-impervious bedrock. Figure 8 shows the general modular concept of STRWARS according to Malet et al (2005), Van Beek et al. (1999), Van Beek (2002), Van Beek et al. (2004). The hydrological model STARWARS uses the embedded meta-language of the pcraster gis package (Wesseling et al., 1996). The full model is built around a core model resolving the dynamic equation for saturated and unsaturated flows and additional sub-models describing specific hydrological processes (Fig. 8a). The model uses measured distributed values for the parameter values. Each layer is represented by a 2-D map (Fig. 8a). Implementation in a GIS-environment has several advantages. First, if based on a high-resolution DEM, the effect of topography can readily be incorporated; secondly, the GIS offers the use of directly available routing functions to define flow paths in each layer. Thirdly, it is possible to include the spatial variation (horizontal and vertical) of the hydrological parameters. This approach provides a unified theoretical description of most of the water fluxes observed within a landslide. The hydrological model consists of three permeable reservoirs (three layers) and an underlying impervious bedrock. The hydrological model describes the saturated and the unsaturated transient flow in the vertical and horizontal directions assuming freely drainable water (Figs. 8a, 8b). Storage and fluxes are considered: antecedent soil moisture in the different reservoirs, infiltration  $I$ , evaporation  $E_p$ , surficial runoff  $R$ , percolation in the unsaturated zone  $P_e$  and saturated lateral flow  $Q_{sat}$  define the hydrological balance of the system. A complete mathematical description of the model can be found in van Beek (2002). For the six test vineyards we used a rudimentary model of STARWARS that was implemented using three different soil depth in order to get information about the spatio temporal dynamics of volumetric soil water content and surface runoff.

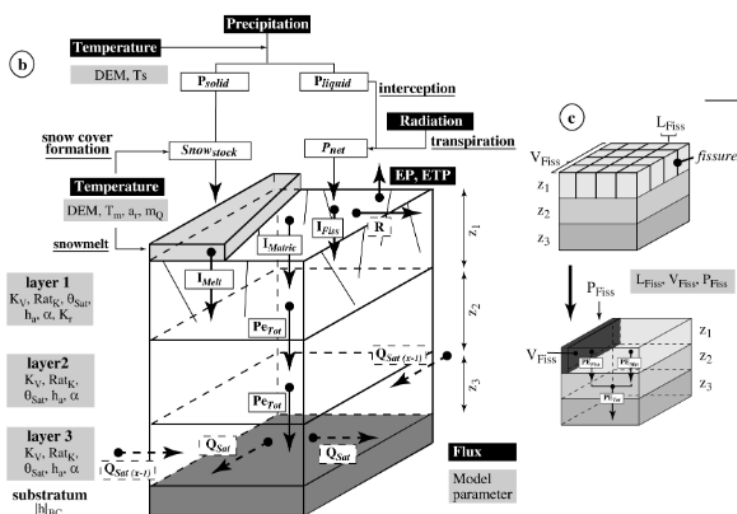
Table 3 reports the main input information for the STARWARS model. The model is set up with constant parameter values, dynamic input with specific time steps and state variables describing the initial state.

Tab. 3. Main STRWARS input data

Model Input		
Constant parameter value	<ul style="list-style-type: none"> <li>Fraction vegetation cover (<math>K_{fac}</math>)</li> <li>Maximum Canopy Storage <math>S_{max}</math> (mm)</li> <li>Correction factor <math>k(-)</math></li> </ul>	<p><b>Global boundary condition</b></p> <ul style="list-style-type: none"> <li>Matric suction for lower boundary <math>[h]_{BC}</math> (m)</li> <li>Matric suction at field capacity, 1<sup>st</sup> layer <math>[h]_{FC}</math> (m)</li> </ul> <p><b>Global land use dependent</b></p> <ul style="list-style-type: none"> <li>Crop factor <math>k_c(-)</math></li> </ul> <p><b>Layer dependent</b></p> <ul style="list-style-type: none"> <li>Saturated hydraulic conductivity <math>k_{sat}</math> (<math>m.d^{-1}</math>)</li> <li>Porosity <math>n</math> (<math>m^3.m^{-3}</math>)</li> <li>Air entry value <math>h_A</math> (m)</li> <li>SWRC slope <math>\alpha(-)</math></li> </ul>
Dynamic Input – All timestep	<ul style="list-style-type: none"> <li>Reference potential evapotranspiration <math>E_{rc}</math> (<math>mm.d^{-1}</math>)</li> <li>Rainfall <math>RF</math> (<math>mm.d^{-1}</math>)</li> </ul>	<p><b>Layer Dependent</b></p> <ul style="list-style-type: none"> <li>Cohesion <math>C</math> (kPa)</li> <li>Angle of Internal Friction <math>\Phi</math> (<math>^\circ</math>)</li> <li>Dry bulk density of soil <math>\gamma_s</math> (<math>kN.m^{-3}</math>)</li> </ul>
Initial condition – state variables	<ul style="list-style-type: none"> <li>Interception <math>I_c</math> (m)</li> <li>Effective Rainfall <math>Eff</math> <math>RF</math> (<math>m.d^{-1}</math>)</li> <li>Remnant of Evapotranspiration to occur from soil <math>E_{rc}</math> Soil (<math>m.d^{-1}</math>)</li> </ul>	<ul style="list-style-type: none"> <li>Effective rainfall <math>Eff</math> <math>RF</math> (<math>m.d^{-1}</math>)</li> <li>Remnant of Evapotranspiration to occur from soil <math>E_{rc}</math> Soil (<math>m.d^{-1}</math>)</li> </ul>
	<ul style="list-style-type: none"> <li>Groundwater level <math>WL</math> (m)</li> <li>Volumetric Soil Moisture Content <math>VMC</math> (<math>m^3.m^{-3}</math>)</li> </ul>	<ul style="list-style-type: none"> <li>Effective degree of saturation (-)</li> <li>Groundwater level <math>WL</math> (m)</li> <li>Factor of Safety <math>F</math> (-) (set to 999, indicating stable initial conditions)</li> </ul>



Parameters	Description
$Kv_1$ ( $cm.d^{-1}$ )*	Saturated vertical conductivity – C1a1
$Kv_2$ ( $cm.d^{-1}$ )*	Saturated vertical conductivity – C1a2
$Kv_3$ ( $cm.d^{-1}$ )*	Saturated vertical conductivity – C1b
$Rat_K$ (-)	Ratio Horizontal/Vertical conductivity
$qSat_1$ (-)*	Porosity value – C1a1
$qSat_2$ (-)*	Porosity value – C1a2
$qSat_3$ (-)*	Porosity value – C1b
$Ha_1$ (m)*	Air entry value – C1a1 (SWRC)
$\alpha_1$ (-)*	Shape factor of the SWRC – C1a1
$ha_2$ (m)*	Air entry value – C1a2 (SWRC)
$\alpha_2$ (-)*	Shape factor of the SWRC – C1a2
$ha_3$ (m)*	Air entry value – C1b (SWRC)
$\alpha_3$ (-)*	Shape factor of the SWRC – C1b
$K_R$ (-)**	Runoff coefficient
$ h _{BC}$ (m)	Matric suction at the bedrock interface



\* layer related parameters  
\*\* estimated by fieldmeasurements

Fig. 8: Architecture of the STARWARS model. ((a) Modular architecture of the model (core model, sub-model) and schematic representation of the model implementation in the pcraster gis package. (b) Representation of the storages and fluxes represented by

the model, and relation between the calculation cells. (c) Schematic representation of the three-parameter conceptual fissure flow model. Definitions of the parameters are listed in Table 2. According to

## Input data preparation

The STARWARS model was set up for the six selected demo farms that show distinct environmental characteristics in terms of morphology, bedrock soils and slope instabilities as reported in table 4.

Table 4: Main settings of the demo farms

Demo farm	Slope angle (°)	Bedrock geology	Soil types (pedological maps at 1:50000 scale)	Soil thickness	Presence of slope instabilities
St. Maria_Ottina-SMV	5-15°	Val Luretta Formation	Calcaric Cambisols	Thin-Medium	No
Vicobarone-VCB	5-15°	Val Luretta Formation	Vertic Cambisols	Very thick	No
Genepreto_Braghi eri-GNP	0-20°	Val Luretta Formation	Vertic Cambisols Endoleptic Regosols	Medium-Very thick	Landslide
Creta_Sartori-CRT	0-10°	Agazzano Subsystem (Alluvial soils)	Silty loams	Very thick	No
Canevino_Piaggi-CNV	10-20°	Varicoloured Clays	Calcaric Cambisols	Thin-Medium	Landslide
Borgopriolo_Dacar ro-BPR	5-15°	S. Agata Fossili Marls	-	-	No

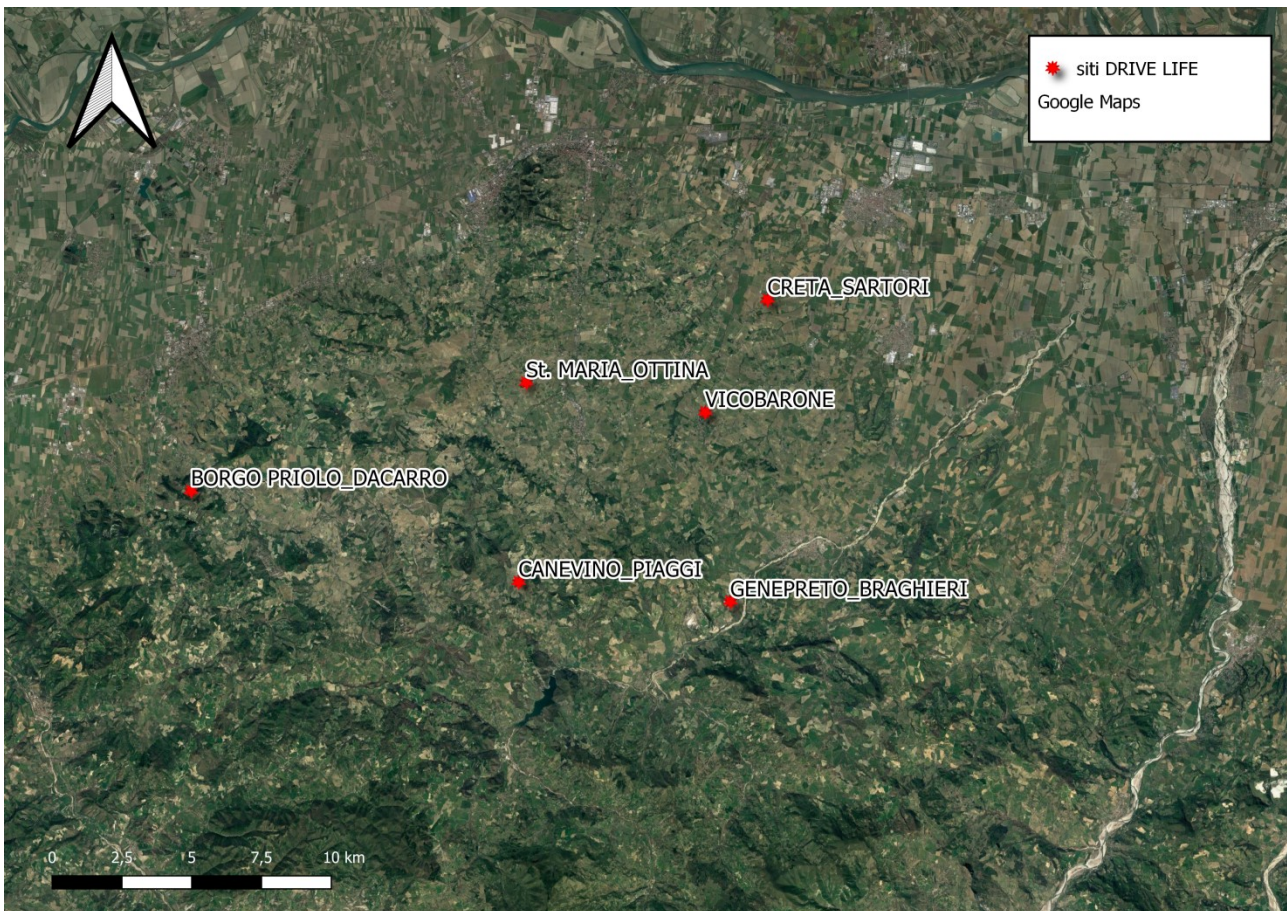


Fig. 9: Map of the demo farms location.

Figure 9 shows the spatial distribution of the demo farms. For the model setup we conducted a detailed field work campaign to get information about the relevant soil parameters. The soils of each demo farm were characterized based on different field and laboratory analyses. After a geophysical survey, conducted in the first months of 2021, two trench pits were opened for each test vineyard. The pits were located along the same inter-row, in the upper and the lower parts of the slopes to highlight possible differences on soil properties due to the different geomorphological position. The pits were averagely 2 m long and 1.5 m large, with variable depth according to the depth of the weathered bedrock. Generally, the pits were dug up to a depth of 1.5-2 m. These surveys were conducted from April to June 2021. For each pit the following analysis were carried out:

- Description of the soil profile, with the identification of soil thickness and of the different diagnostic horizons.
- Collection of undisturbed samples, for each identified horizon, for the laboratory analysis allowing to derive the following parameters: soil texture (sand, silt, and clay percentages)
- Collection of undisturbed samples, each 10 cm along the soil profile, for the physical laboratory analysis of soil volumetric features (unit weight, dry density, porosity, void index, water content, saturation degree)
- Collection of undisturbed soil samples, for the representative soil horizons generally located between 0.2 and 0.7 m from ground level, for the determination of the soil water retention curve.

The general soil characterization was completed with the measures of soil hydraulic conductivity in field, at different depths along the soil profile, in the period between June and July 2021. Soil hydraulic conductivity

were measured in different positions along the slopes of the test vineyards and in correspondence of inter-rows where different management practices are applied. For each site K-Sat measurements were conducted using a compact constant head permeameter (Amoozemeter; /Amoozegar, 1989). The measurements were conducted in the period July 2021. The saturated hydraulic conductivity on the topsoil (0-20cm) and subsequently in the subsoil (20-40) was measured for the interrows of each land use type characterizing the vineyard.

According to the soil analysis that in detail is described in the “Report on chemical-physical features and hydraulic properties of selected vineyard soils, Sub-action B2.1 Starting point and road map to selection of most suited resilience practices” we differentiated and implemented the model using three soil horizons distinguishing between topsoil, subsoil and underlying substrates using the following depth ranges:

- <25cm Topsoil
- 25-80cm Subsoil
- 80-120cm Substrate

A part of the soil information we also characterized the row management for the vegetational parameters relevant for the evapotranspiration calculations as reported in table 5.

Table 5. List of the implemented management practices in demo farms.

Demo farm	Management
SMV	Control
	Green manure High
	Green manure medium
	Green manure low
VCB	Nitrofert
	Control
	Humusfert
	Stratus
GNP	Control
	Nitrofert
	Stratus
CRT	Control
	Rolling
	Swath
CNV	Humusfert
	Control
BPR	Stratus
	Control
	Nitrofert

The climatic data and the soil moisture information is retrieved by the automatic climate and soil moisture monitoring stations implemented in the period April-May 2021. In each demo farm, the probes for the measure of the meteorological parameters were installed in correspondence of a station, which is connected remotely with different monitoring points of the soil hydrological parameters installed in the test vineyards (for details see Report on activity B2 “Report on chemical-physical features and hydraulic properties of selected vineyard soils”, Sub-action B2.1). As climatic input for the STARWARS model we use information about solar radiation. Rainfall, temperature. Soil moisture data is used to calibrate and validate the model application.

The topographic data input for the STARWARS model is based on a high-resolution digital elevation model based on LIDAR data that was resampled on 2m resolution. We used SAGA GIS to do the preprocessing (artefact removal and fill sink procedure) and the delineation of the respective catchment of the selected vineyards. Fig. 10 shows the catchment of the selected Canevino demo farm vineyard.

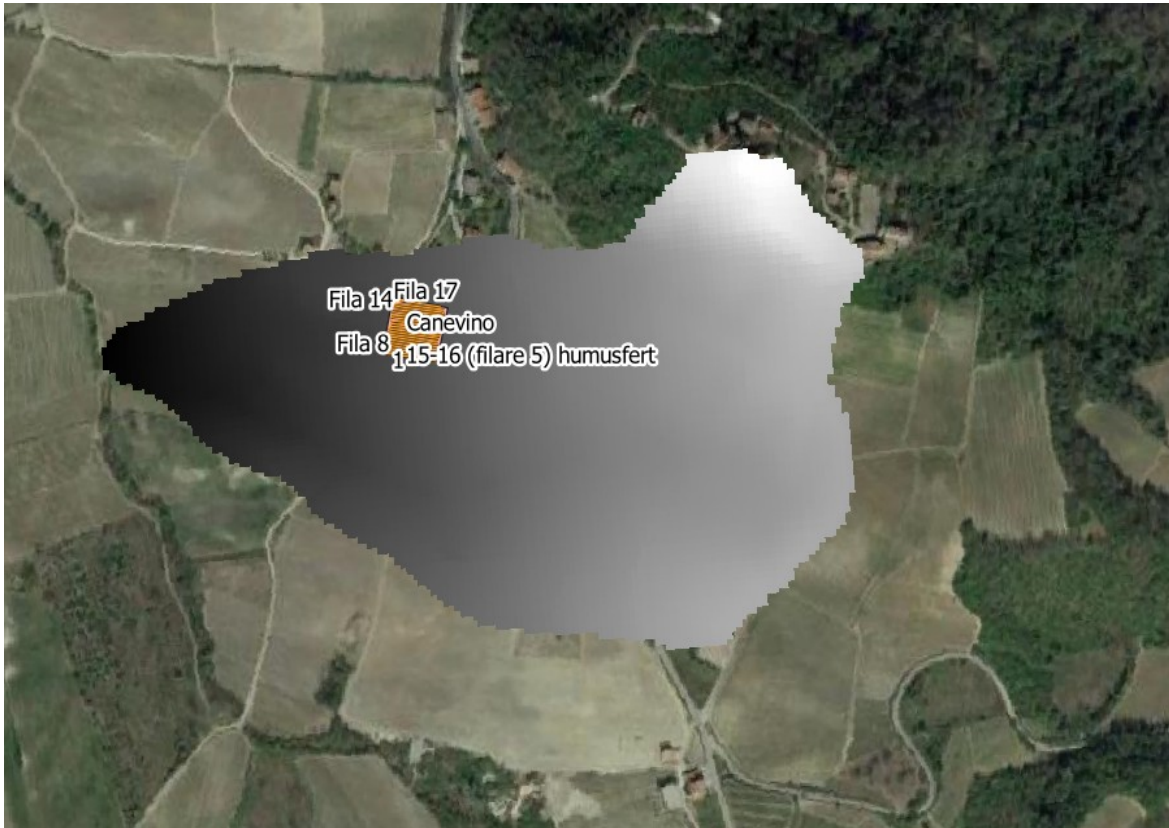


Fig.10: Canevino Demo Farm with the respective catchment of the selected vineyard

## Model calibration

The Starwars model was calibrated using the proposed procedure by Saxton and Rawls (2006) considering soil texture information and soil organic matter content. Therefore, statistical analyses were conducted using measured soil water properties for the analysed soils. Prediction equations were derived for soil moisture tensions of 0, 33, and 1500 kPa and air-entry based on the available variables of soil texture and organic matter (see Fig. 11). The latter were combined with equations of conductivity, to provide a water characteristic model useful for a wide range of soil water and hydrologic applications. Figure 12 shows the model calibration runs for the soil water content and the three soil depths. As shown in Fig. 12 the modelled and available measured data fit quite well for this first calibration runs.

## Model results

Fig. 13 illustrates the dynamic volumetric soil water content (VMC) values over time visualized using the STARWARS dynamic output tool. The values can be retrieved for each single 2x2m pixel of the DEM. The results can be also exported in textfile format reporting the pixel coordinates, the respective interrow management, the volumetric water content for each of the selected three soil depth as well as the respective rainfall, surface runoff and calibration parameters. VMC values fit well with the distinguished top soil layer but



perform relatively poor in the mid-soil layer. For better calibration results at all selected sites, the outcomes suggest to modify the pedohydraulic parameters of the lithic boundary conditions (or what is defined as bedrock in the model). However, the outcomes reflect an overall acceptable performance of the model and it is expected that VMC-values for all selected sites can be reproduced in a reliable manner.

Parameter distributions and tested values for calibration at CNV 1 and 2

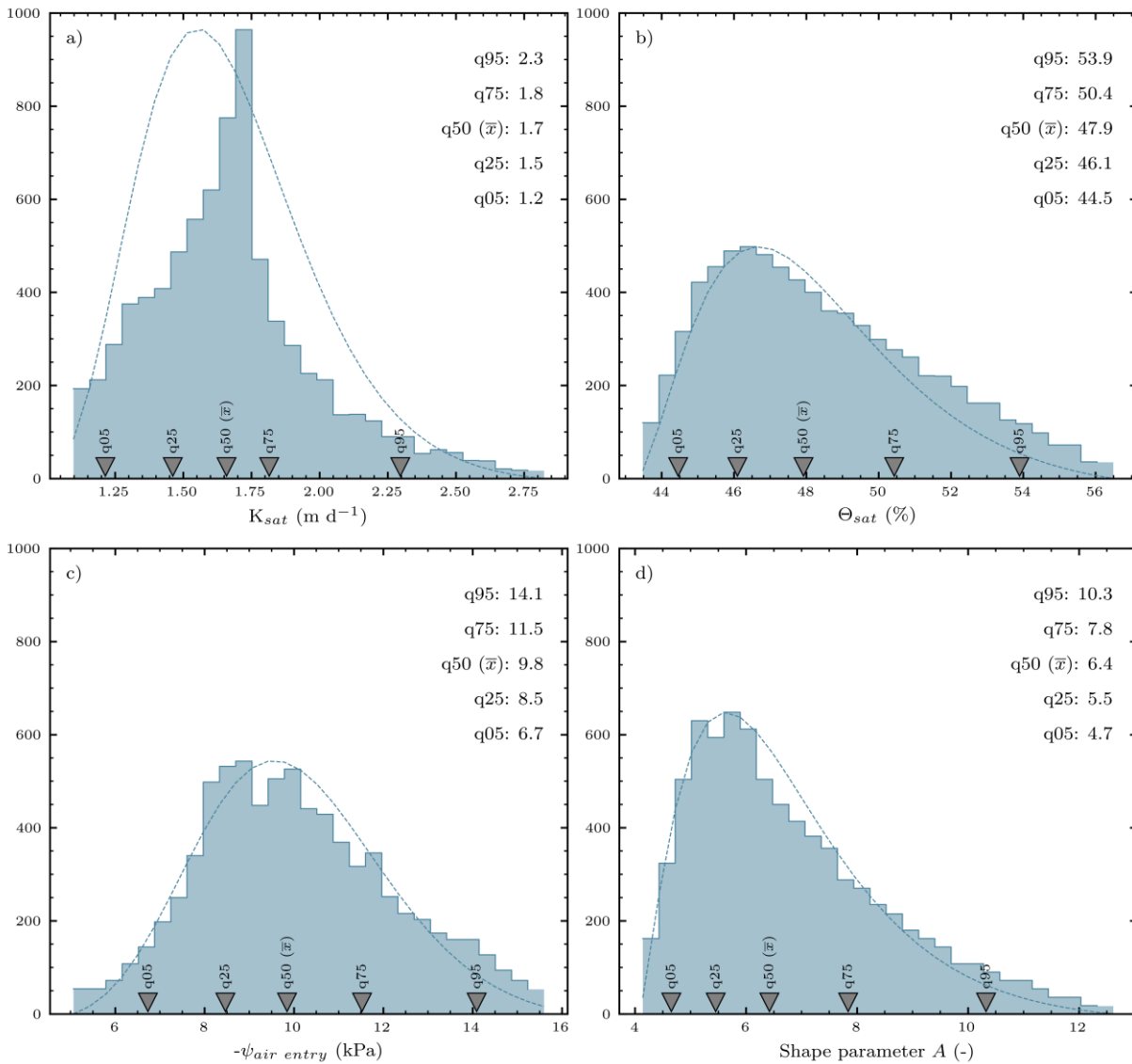


Figure 11: Parameter distribution and tested values for calibration of Canevino 1 and 2

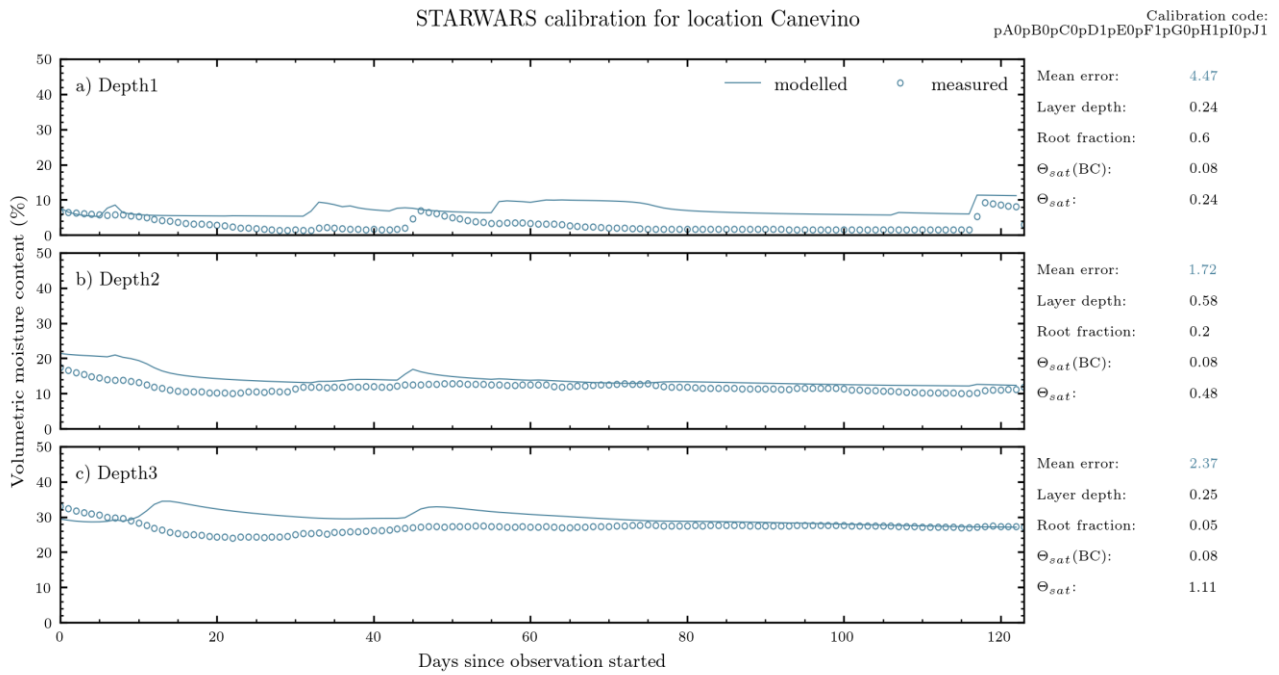


Figure 12: Calibration model runs for Canevino using volumetric moisture content (%)

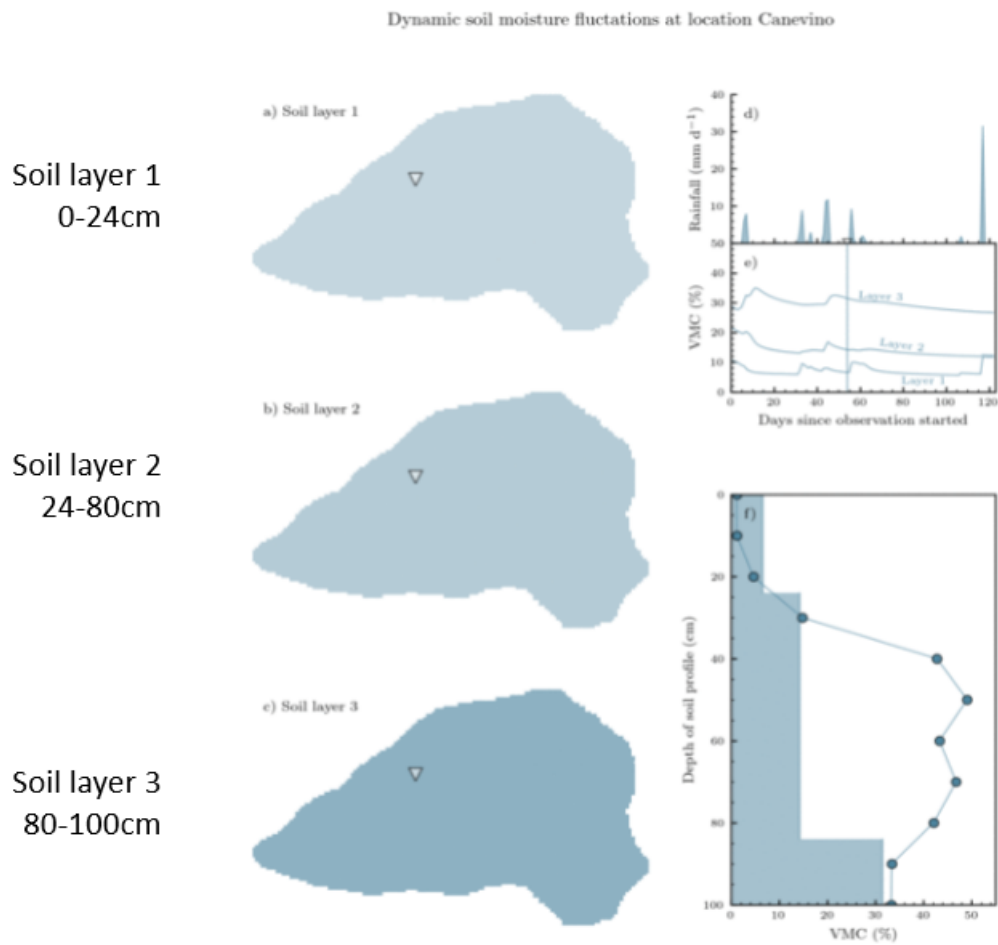


Figure 13: Tool showing the dynamic soil moisture distribution for the Canevino demo farm

## References

- Baret, F.; de Solan, B.; Lopez-Lozano, R.; Ma, K.; Weiss, M., 2010. GAI estimates of row crops from downward looking digital photos taken perpendicular to rows at 57.5 zenith angle: Theoretical considerations based on 3D architecture models and application to wheat crops. *Agricultural and Forest Meteorology*, 150, 1393–1401.
- Bellvert, J., Zarco-Tejada, P.J., Girona, J., Fereres E., 2014. Mapping crop water stress index in a 'Pinot-noir' vineyard: comparing ground measurements with thermal remote sensing imagery from an unmanned aerial vehicle. *Precision Agriculture*, 15,361–376.
- Campbell, G.S., 1986. Extinction coefficients for radiation in plant canopies calculated using an ellipsoidal inclination angle distribution. *Agricultural and Forest Meteorology*, 36, 317–321.
- Campbell, G.S., 1990. Derivation of an angle density function for canopies with ellipsoidal leaf angle distributions. *Agricultural and Forest Meteorology*, 49, 173–176.
- Campos-Taberner, M., García-Haro, J., Confalonieri, R., Martínez, B., Moreno, Á., Sánchez-Ruiz, S., Gilabert, M.A., Camacho, F., Boschetti, M., Busetto, L., 2016. Multitemporal monitoring of plant area index in the Valencia rice district with PocketLAI. *Remote Sensing*, 8, 202-17.
- Confalonieri, R., Foi, M., Casa, R., Aquaro, S., Tona, E., Peterle, M., Boldini, A., De Carli, G., Ferrari, A., Finotto, G., Guarneri, T., Manzoni, V., Movedi, E., Nisoli, A., Paleari, L., Radici, I., Suardi, M., Veronesi, D., Bregaglio, S., Cappelli, G., Chiodini, M.E., Dominoni, P., Francone, C., Frasso, N., Stella, T., Acutis, M., 2013. Development of an app for estimating leaf area index using a smartphone. Trueness and precision determination and comparison with other indirect methods. *Computers and Electronics in Agriculture*, 96, 67-74.
- Francone, C., Pagani, V., Foi, M., Cappelli, G., Confalonieri, R., 2014. Comparison of leaf area index estimates by ceptometer and PocketLAI smart app in canopies with different structures. *Field Crops Research*, 155, 38-41.
- Orlando, F., Movedi, E., Coduto, D., Parisi, S., Brancadoro, L., Pagani, V., Guarneri, T., Confalonieri, R., 2016. Estimating LAI in vineyard using the PocketLAI smart-app. *Sensors*, 16, 2004.
- Williams, L.E., Araujo, F.J., 2002. Correlations among predawn leaf, midday leaf, and midday stem water potential and their correlations with other measures of soil and plant water status in *Vitis vinifera*. *Journal of the American Society for Horticultural Science*, 127, 448–454.
- Allen R.G., Pereira L.S., Raes D., Smith M., 1998. Crop evapotranspiration—guidelines for computing crop water requirements—FAO irrigation and drainage paper 56. FAO—Food and Agriculture Organization of the United Nations, Rome, Italy.
- Calò A., Costacurta A., Tomasi D., Biscaro S., 1997. La fenologia della vite in Italia in rapporto alle condizioni ambientali. in Calò A. (ed): il determinismo climatico sulla fenologia della vite e la maturazione dell'uva in Italia. *Arti Grafiche. Conegliano (TV)*, 14-15 luglio 93, p. 3-71.
- Cola G., Failla O., Maghradze D., Megreldze L., Mariani L., 2017. Grapevine phenology and climate change in Georgia. *International Journal of Biometeorology*, 61, 761-773.
- Cola G., Mariani L., Salinari F., Civardi S., Bernizzoni F., Gatti M., Poni S., 2014. Description and testing of a weather-based model for predicting phenology, canopy development and source-sink balance in *vitis vinifera* L. cv. Barbera. *Agricultural and Forest Meteorology*, 184, 117-136.
- Mariani M., Alilla R., Cola G., Dal Monte G., Epifani C., Puppi G., Failla O., 2013. IPHEN-a real-time network for phenological monitoring and modelling in Italy. *International Journal of Biometeorology*, 57, 881-893.
- Meier U., 2003. Phenological growth stages. In: Schwartz M.D. (ed.), *Phenology: an integrative science*. Kluwer Academic, The Netherlands, pp. 269–283.
- Riou C., Valancogne C., Pieri P., 1989. Un modele simple d'interception du rayon-nement solaire par la vigne. Vérification expérimentale. *Agronomie* 9, 441–450.

## STARWARS Model Application refernces

- Jean-Philippe Malet, Th. W. J. van Asch, R. van Beek, O. Maquaire (2005): Forecasting the behaviour of complex landslides with a spatially distributed hydrological model. *Natural Hazards and Earth System Sciences, Copernicus Publ. / European Geosciences Union*, 5 (1), pp.71-85.
- Sexton K.E. and W.J. Rawls (2006): Soil Water Characteristic Estimates by Texture and Organic Matter for Hydrologic Solutions. *SSSAJ*, 70(5), 1569-1578. <https://doi.org/10.2136/sssaj2005.0117>
- Van Beek, L. P. H.(2002): Assessment of the influence of changes in land use and climate on landslide activity in a Mediterranean environment, PhD Thesis, University of Utrecht, Netherlands, 2002.
- Van Beek, L. P. H. and Van Asch, T. W. J. (1999): A combined conceptual model for the effects of fissure-induced infiltration on slope stability, in: *Process Modelling and Landform Evolution, Lect. Notes Earth Sci.*, 78, 147–167, doi:10.1007/BFb0009716.
- Van Beek, L. P. H. and Van Asch, Th. W. J. (2004): Regional assessment of the effects of land-use change on landslide hazard by means of physically based modelling, *Nat. Hazards*, 31, 289–304.

Wesseling C.G., Van Deursen W.P.A., Burrough P.A. (1996): A spatial modelling language that unifies dynamic environmental models and GIS. Third International Conference/Workshop on Integrating GIS and Environmental Modeling. <http://pcraster.geog.uu.nl/publications.htm>